NOAA Technical Memorandum EDS BOMAP-15

PARAMETERIZED MOISTURE AND HEAT FLUX THROUGH TOP OF BOMEX VOLUME

Vance A. Myers

Washington, D.C.
May 1975

noaa NATIONAL OCEANIC AND ATMOSPHERIC ADMINISTRATION / Environmental Data Service

NOAA TECHNICAL MEMORANDA

Environmental Data Service, BOMAP Series

The Barbados Oceanographic and Meteorological Experiment (BOMEX) was conducted in May, June, and July 1969. Following the field experiment, the Barbados Oceanographic and Meteorological Analysis Project (BOMAP) was established in the Research Laboratories (ESSA), now NOAA, to coordinate the reduction of the data collected; to analyze these data, particularly those pertaining to the Sea-Air Interaction Program (the BOMEX Core Experiment); and to provide a central contact point for information exchange and publication of BOMEX results.

The name of the BOMAP Office was subsequently changed to Center for Experiment Design and Data Analysis (CEDDA), which was transferred to NOAA's Environmental Data Service in 1972. BOMAP remains, however, one of CEDDA's responsibilities, and publication of NOAA Technical Memoranda will continue as a means for disseminating information resulting from analyses of BOMEX data conducted at CEDDA. ERLTM-BOMAP-1 was published in the series of ESSA Technical Memoranda, ESSA Research Laboratories. ERL BOMAP-2 through ERL BOMAP-9 were issued as part of the series of NOAA Technical Memoranda, Environmental Research Laboratories. Subsequent publications are part of the series of NOAA Technical Memoranda, Environmental Data Service.

Publications listed below are available from the National Technical Information Service, U.S. Department of Commerce, Sills Bldg., 5285 Port Royal Road, Springfield, Va. 22151. Price: Paper copy prices vary; $1.45 for microfiche. Order by accession number shown in parentheses at end of each entry.

ESSA Technical Memoranda

ERLTM-BOMAP 1 High-Level Cloud Photography Inventory, BOMEX Period IV, July 11-28, 1969. Vance A. Myers, September 1970, 66 p. (PB-194-661)

NOAA Technical Memoranda

ERL BOMAP-2 A Statistical Data Plan for BOMEX. Theodore W. Horner, December 1970, 105 p. (COM-71-00188)

ERL BOMAP-3 Mass, Momentum, and Energy Budget Equations for BOMAP Computations. Eugene M. Rasmusson, January 1971, 32 p. (COM-71-00195)

ERL BOMAP-4 High-Level Cloud Photography Inventory, BOMEX Period II, May 24-June 10, 1969. Vance A. Myers, March 1971, 86 p. (COM-71-00574)

ERL BOMAP-5 Preliminary Velocity Divergence Computations for BOMEX Volume Based on Aircraft Winds. Robert W. Reeves, April 1971, 21 p. (COM-71-00667)

ERL BOMAP-6 Ship's Influence on Surface and Rawinsonde Temperatures During BOMEX. Warren M. Wisner, June 1971, 44 p. (COM-71-00950)

ERL BOMAP-7 High-Level Cloud Photography Inventory, BOMEX Period I, May 3-15, 1969. Vance A. Myers, December 1971, 55 p. (COM-72-10196)

ERL BOMAP-8 BOMEX Flight Tracks Reconstructed From Near-Simultaneous High-Level Cloud Photography by Two Aircraft. Vance A. Myers and Martin Predoehl, December 1971, 13 p. (COM-72-10313)

ERL BOMAP-9 The BOMEX Sea-Air Interaction Program: Background and Results to Date. Joshua Z. Holland, March 1972, 34 p. (COM-72-10576)

EDS BOMAP-10 BOMEX Rainy Day Analysis. Lt. Garry W. Elliott, July 1973, 9 p. (COM-74-10466)

EDS BOMAP-11 Method for Obtaining Wet-Bulb Temperatures by Modifying the Psychrometric Formula. J. Sullivan and L. D. Sanders, June 1974. (COM-74-11425/AS)

EDS BOMAP-12 Profiles in the Lowest 300 Meters of the Marine Tropical Planetary Boundary Layer. C. F. Ropelewski, September 1974, 24 pp. (COM-74-11779/AS)

EDS BOMAP-13 Water-Vapor and Mass Divergence Computations Based on BOMEX Aircraft and Rawinsonde Data: A Comparison. Robert W. Reeves, December 1974. (COM-75-10268)

EDS BOMAP-14 Geostrophic Motion for the BOMEX Oceanic Volume. Victor E. Delnore, in press, 1975.

NOAA Technical Memorandum EDS BOMAP-15

PARAMETERIZED MOISTURE AND HEAT FLUX THROUGH TOP OF BOMEX VOLUME

Vance A. Myers

Washington, D.C.
May 1975

UNITED STATES
DEPARTMENT OF COMMERCE

NATIONAL OCEANIC AND
ATMOSPHERIC ADMINISTRATION
Robert M. White, Administrator

Environmental Data
Service
Thomas S. Austin, Director

CONTENTS

	Page
Notation	v
Abstract	1
1. Introduction	1
2. Cloud and Clear-Air Components of Moisture Flux Through Top of BOMEX volume	2
2.1 Cloud Moisture Flux	2
2.2 Clear-Air Moisture Flux	3
3. Convective Chimney Model	4
3.1 Steady-State Stage	4
3.2 Growth Stage	5
4. Dimensionless Ratios of Moisture Flux to Rainfall	5
4.1 Steady-State Tall Chimney	6
4.2 Steady-State Medium-Size Chimney	8
4.3 Growth Stage	9
5. Mass Flux Ratio	12
6. Enthalpy Flux	14
6.1 Clear-Air Flux	15
6.2 Cloud Flux	15
6.3 Total Flux	16
7. Cloud Parameters	18
7.1 Representative Environmental Clear-Air Sounding	18
7.2 Cloud Temperature	19
7.3 Mean Inflow Specific Humidity, $\overline{q}^{+}$	23
7.4 Cloud Water, Q	23
7.5 Pressure at Top of BOMEX Volume	23
7.6 Height Vs. Pressure	23
7.7 Mean Outflow Specific Humidity, $\overline{q}^{-}$	23
7.8 Cloud Height	26
7.9 Influence of Cloud Parameters on Moisture Flux Ratio	26
8. Cloud Height Effects: Application of Radar Data	29
8.1 Moisture Flux Ratio Vs. Cloud Height	29
8.2 Cloud Height Vs. Rainfall Rate From Radar	32
8.3 Moisture Flux Ratio Vs. Rainfall Rate	32

CONTENTS

(continued)

Page

8.4 Significant Rainfall Rates 35
8.5 Recommendation 36

9. Fluxes Through the Top of the BOMEX Volume Per Millimeter of Rainfall 36

9.1 Moisture Flux 36
9.2 Mass Flux 37
9.3 Vertical Velocity 37
9.4 Enthalpy Flux 37

Acknowledgements 38

References 38

NOTATION

Averages

Averages are denoted by a bar followed by one or more letters that are indices identifying the character of the average. For example, $\overline{}^{t}$ denotes an average over time. Other averaging indices in this report are

a = portion of B outside clouds

B = area of BOMEX square on a p* surface

c = portion of B within clouds

k = portion of B within particular cloud chimney of serial number k

T = top of BOMEX volume (p* = 500 mb)

+ = over portion of surface of cloud chimney where V_n is inward (see sec. 5)

− = over portion of surface of cloud chimney where V_n is outward (see sec. 5).

Deviations From Averages

Deviations from averages are denoted by parentheses followed by one or more of the above letter indices as a superscript. For example, $(\ )^{cT}$ means local deviation from the areal average over the cloudy portion of the surface of the top of the BOMEX volume. Exponents are not used following parentheses. All other superscripts are conventional exponents.

Variables	Units
A = area, either horizontally or on p* surface	(cm^2)
C = perimeter around convective chimney at p* = constant	(cm)
c_p = specific heat of air at constant pressure	(cal gm^{-1} deg^{-1})
E = evaporation rate at sea surface	(gm cm^{-2} s^{-1})
F_H = enthalpy flux	(cal cm^{-2} s^{-1})
F_w = flux of water substance	(gm cm^{-2} s^{-1})
F_x = flux of X	(X cm^{-2} s^{-1})
g = acceleration of gravity	(cm s^{-2})
L = latent heat of vaporization	(cal gm^{-1})

M	= vertical mass transport	(gm s^{-1})
P	= precipitation rate	(gm cm^{-2} s^{-1})
p	= pressure	(microbars)
p*	= pressure difference	(microbars)
PR	= Radar maximum power return (same as $\overline{P}_{rm}$, Hudlow, 1971)	(μW)
q	= specific humidity (of water vapor)	(gm gm^{-1})
Q	= cloud water and ice concentration in specific humidity units	(gm gm^{-1})
R	= rain water concentration in specific humidity units	(gm gm^{-1})
S	= surface of convective chimney	(cm^2)
T	= temperature, Kelvin (except Celsius in figs. 3 to 6)	(deg)
T_d	= dewpoint, Celsius	(deg)
V	= speed	(cm s^{-1})
W	= weight in averaging variables	(dimensionless)
X	= any scalar quantity	
ρ	= density	(gm cm^{-3})
ω*	= dp*/dt	(microbars s^{-1})
ΔT	= excess of cloud temperature over environmental temperature at same pressure	(deg)
ΔT'	= effective ΔT (see sec. 7)	(deg)
τ	= potential pseudo-wet-bulb temperature (same as θ_{sw} in standard texts), Celsius	(deg)

Subscripts

a = outside cloud chimneys (B exclusive of c)

b = base of outflow layer

B = BOMEX square

c = within cloud chimneys

e = immediate environment of cloud chimneys

H = enthalpy

i = top of inflow layer

k = serial number of cloud chimney

n = normal to exterior boundary of a cloud chimney, positive outward

o = at sea-air interface

s = saturated

T = top of BOMEX volume

w = water substance, gas plus liquid

x = any quantity

z = top of convective chimney, steady state; ultimate top, growth stage

PARAMETERIZED MOISTURE AND HEAT FLUX THROUGH TOP OF BOMEX VOLUME

Vance A. Myers*
Office of Hydrology, National Weather Service
National Oceanic and Atmospheric Administration
Silver Spring, Md. 20910

Abstract: A prime objective of the Barbados Oceanographic and Meteorological Experiment (BOMEX) in 1969 was to determine the budgets of moisture, enthalpy, and mass in a fixed atmospheric volume over a tropical ocean. The fluxes through the top of the volume, approximately at 500 mb, were not measured directly. A parameterization scheme is developed to estimate the top-of-volume moisture flux as a ratio to rainfall produced. The enthalpy flux is also treated briefly.

1. INTRODUCTION

The observational program of the Barbados Oceanographic and Meteorological Experiment (BOMEX), designed by Davidson (1968) and conducted in the summer of 1969 east of Barbados, has been described in detail in BOMEX Field Observations and Basic Data Inventory (BOMAP Office, 1971). Rawinsonde and aircraft measurements of wind, specific humidity, and temperature were made in May and June 1969 over a 500-km by 500-km square array to determine the lateral fluxes through the sides of the BOMEX volume in support of the BOMEX Core Experiment. The primary aim was to estimate the evaporation rate from the ocean to the atmosphere by accounting for all other moisture fluxes into and out of a specific volume and thereby infer the evaporation rate as a residual (Holland and Rasmusson, 1973). This is the budget approach to assessing atmospheric behavior. The energy budget was also analyzed, leading to inferences on the sensible heat interchange between the ocean and atmosphere and the energy conversions within the volume.

In their study, Holland and Rasmusson reported results of a trial analysis of the atmospheric budgets of mass, water vapor, heat, momentum, and mechanical energy based on rawinsonde data for a 5-day period of relatively undisturbed trade-wind weather. Other analyses are in progress of sequences of disturbed days, for which rainfall to the sea surface and the liquid and vapor flux through clouds that penetrate the top of the BOMEX volume (~500 mb) are more critical terms in the moisture budget. The experimental design for estimating rainfall for these analyses rests on the use of radar data supplemented by satellite observations (Hudlow 1970, 1971; Scherer and Hudlow 1971, 1975).

*Former affiliation: Center for Experiment Design and Data Analysis, EDS, NOAA.

In this paper, a method is developed for estimating the cloud flux term in the Core Experiment moisture budget. This term is parameterized as a ratio to rainfall rate, and the cloud mass and enthalpy fluxes through the top of the BOMEX volume are also keyed to rainfall. Specific applications of the formulations developed are indicated.

2. CLOUD AND CLEAR-AIR COMPONENTS OF MOISTURE FLUX THROUGH TOP OF BOMEX VOLUME

The top of the BOMEX volume is coincident with the 500-mb surface in the pressure difference, or p*, system, where p* is the position on the vertical axis in terms of pressure differential relative to sea level, i.e., p* = 0 at sea level (Rasmusson, 1971). The flux of any quantity X through this surface and averaged over the area of the surface, $\overline{F_x}^{BT}$, is the sum of the within-cloud average flux and the clear-air average flux, weighted by their respective fractional parts of the total area:

$$\overline{F_x}^{BT} = \frac{A_c}{A_B} \overline{F_x}^{cT} + \left(1 - \frac{A_c}{A_B}\right) \overline{F_x}^{aT} \quad . \tag{1}$$

The cloud flux in turn is the sum of the mean fluxes in individual clouds weighted by the respective cloud areas at the top of the BOMEX volume:

$$\overline{F_x}^{cT} = \frac{1}{A_c} \sum_{k=1}^{n} A_k \overline{F_x}^{kT} \quad , \tag{2}$$

where the subscript k refers to individual clouds and n is the total number of clouds.

2.1 Cloud Moisture Flux

The moisture flux in clouds has three components: water vapor; cloud water, assumed to move with the air; and rainfall, assumed to fall at its own terminal velocity. Thus if X is the moisture concentration,

$$X = q + Q + R \quad . \tag{3}$$

The net moisture flux through the top of the BOMEX volume within the kth cloud is then

$$\overline{F_w}^{kT} = \frac{\overline{q\omega^*}^{kT}}{g} + \frac{\overline{Q\omega^*}^{kT}}{g} - \overline{P}^{kT} \quad , \tag{4}$$

and the mean moisture flux for the entire cloudy area is

$$\overline{F_w}^{cT} = \frac{1}{A_c} \sum_{k=1}^{n} A_k \, \overline{F_w}^{kT} \quad . \tag{5}$$

The largest part of this report is devoted to evaluating eq. (4) and thereby eq. (5).

2.2 Clear-Air Moisture Flux

The mean clear-air moisture flux is simply the mean of the product of vertical flux of mass ω^*/g and the specific humidity:

$$\overline{F_w}^{aT} = \frac{\overline{q\omega^*}^{aT}}{g} \quad . \tag{6}$$

Of necessity we ignore the covariance term and approximate the mean product by the product of the means:

$$\overline{F_w}^{aT} = \frac{1}{g} \, \overline{q}^{aT} \, \overline{\omega^*}^{aT} + \frac{1}{g} \, \overline{(q)^{aT}(\omega^*)^{aT}} \approx \frac{1}{g} \, \overline{q}^{aT} \, \overline{\omega^*}^{aT} \quad . \tag{7}$$

This is probably not a serious omission under BOMEX conditions. It is evident from results reported by Holland and Rasmusson (1973) that the microscale flux is small at the level of the top of the volume, and the mesoscale flux is not very large, either.

The mean clear-air specific humidity $\overline{q}^{aT}$ in (7) is approximated by averaging values obtained from radiosonde soundings at appropriate times. The mean clear-air vertical velocity $\overline{\omega^*}^{aT}$ must be calculated from the mass balance. The mass budget, unlike the moisture and enthalpy budgets, has no component through the bottom of the atmospheric portion of the BOMEX volume (the sea surface); therefore, knowing the flux through the sides of the volume, the mean mass flux rate through the top of the volume, $\overline{\omega^*/g}^{BT}$, can be calculated from mass continuity, as has been done by Holland and Rasmusson (1973). This flux is then partitioned by eq. (1):

$$\frac{1}{g} \, \overline{\omega^*}^{BT} = \frac{1}{g} \, \frac{A_c}{A_B} \, \overline{\omega^*}^{cT} + \frac{1}{g} \left(1 - \frac{A_c}{A_B}\right) \overline{\omega^*}^{aT} \quad . \tag{8}$$

The mean vertical mass flux within clouds, $\overline{\omega^*/g}^{cT}$, must be parameterized along with the cloud moisture and enthalpy fluxes in terms of cloud population and parameters. When this is done, there is but one unknown remaining in eq. (8), namely $\overline{\omega^*/g}^{aT}$, which in turn can be inserted in (7), leading to a solution for the clear-air moisture flux, $\overline{F_W}^{aT}$.

3. CONVECTIVE CHIMNEY MODEL

The BOMEX radar program identifies the radar echo population and estimates the heights and precipitation yields of the respective echoes (Hudlow, 1971). Satellite data are used as a means of extrapolating rainfall estimates to areas of the BOMEX square not covered by radar data (Scherer and Hudlow, 1971, 1975). Thus the locations, areal extent, heights (in a statistical sense), and precipitation yields are given quantities available for estimating fluxes at the top of the BOMEX volume. In this section, we present the set of assumptions constituting our proposed model.

Conceptually, we place a vertical wall along the edges of each isolated radar echo, or along the collective perimeter of a group of closely spaced echoes. This vertical wall, the sea surface, and a p* surface tangent to the top of the echo, bound a volume that we will call a convective chimney. This chimney is intermediate in scale between an individual cloud and the cloud grouping that has come to be called a "cloud cluster" in tropical meteorology dynamics.

All within-chimney quantities are averaged areally on a p* surface, as are the surface fluxes. Lateral boundary fluxes are averaged along a perimeter surrounding such a surface. Some quantities are also averaged in the vertical between p* surfaces.

The fully developed convective chimney is modeled in a steady state, which yields most of the rain. This is preceded by a growth stage, with accompanying lesser rainfall volume. In the subsequent decay stage, precipitation and fluxes are insignificant and are not considered here.

3.1 Steady-State Stage

Mass Flow. During the mature steady-state stage, environmental air enters the sides of the lower part of the convective chimney (including the sides below visible cloud base), rises vertically, and exits through the sides of the upper part of the chimney. There is no flow through the top, which has been placed at the $\omega^* = 0$ level. We will refer to the lower inflow layer, the upper outflow layer, and the nondivergent layer, the intermediate region of no lateral exchange.

Water States and Transport. The inflow carries environmental water vapor into the cloud chimney at the specific humidity q_a of the environment. Additional water vapor evaporates from the sea surface at rate E, but we will mostly neglect this because within convective chimneys it is small compared

with precipitation P. Throughout the portion of the convective chimney volume above cloud base, saturation specific humidity q_s prevails, and cloud water and/or ice with concentration Q is present. Both move with the air motion within the cloud and are carried out of the chimney volume by the outflow. Condensation in excess of $q_s + Q$ becomes rain and falls vertically. Steady-state conservation of moisture requires that the lateral inflow of water vapor plus evaporation exactly equal the lateral outflow of vapor and cloud water or ice plus flux of rain through the base of the chimney (sea surface). There is no transport through the top surface of the chimney, which has been placed at the level where $\omega^* = 0$.

Lapse Rate. In the lower part of the cloud the temperature lapse rate is slightly in excess of the saturation adiabatic, as dictated by steady-state lateral entrainment of unsaturated air. The limiting lapse rate for zero entrainment is the saturation adiabatic; thus the saturation adiabatic lapse rate prevails in the nondivergent and outflow layers.

Energy Conservation. In the nondivergent and outflow layers the equivalent potential temperature is constant with height. Conservation of energy requires that the mean transport-weighted equivalent potential temperature of the inflow air equal this value. This fact is important in parameterizing the bounds of the inflow layer (sec. 7).

Buoyancy. Buoyancy is not explicitly evaluated in this model. It is implicitly assumed that the vertical equation of motion is satisfied, and that, level for level, either cloud air density differs only slightly from environmental density or that, if large density differences do exist, the cloud overshoots at the top and reaches a level where it is more dense than the environment. We presume that our chosen cloud heights, being derived from real clouds, introduce these conditions.

3.2 Growth Stage

The transition of a nonprecipitating group of cumulus clouds to an effective rain-producing convective chimney is simulated by the following model. Inflow into the convective chimney volume is the same as during the subsequent steady-state stage. The inflow air moves upward like a piston within the volume. When the face of the piston (cloud top) passes some assigned threshold level, rain begins. This is time $t = 0$. The piston continues to the top of the volume, reaching it at time $t = t_z$. The steady-state stage then begins. The air above the piston during the growth stage exits horizontally without contributing to precipitation or vertical flux. Below the face of the piston the lapse rate is the same as in the steady state (saturation-adiabatic or slightly steeper), and condensation in excess of $q_s + Q$ falls as precipitation.

4. DIMENSIONLESS RATIOS OF MOISTURE FLUX TO RAINFALL

The net moisture flux through the top of the BOMEX volume in a given convective chimney will be expressed as the ratio to the rainfall rate through the base of the chimney, that is, at sea level.

Conceive of the convective chimneys as grouped into three size categories: tall chimneys, in which the entire convergent inflow is below the level of the top of the BOMEX volume, the flow is nondivergent at the top, and the entire outflow is above the top (fig. 1,p.11); medium chimneys, in which the entire inflow is below the top of the BOMEX volume, but a portion of the outflow is also below the top, and short chimneys, which do not reach to the top of the volume and do not contribute to the flux through it.

4.1 Steady-State Tall Chimney

Moisture Flux Ratio. The moisture conservation equation for a steady-state convective chimney can be expressed as an integral over the surface of the volume:

$$\int_{S_k} (V_n \rho q + V_n \rho Q + P - E)\, dS = 0 \quad , \tag{9}$$

where V_n is the component of air motion normal to the surface positive outward, and ρ is density. Since there is no air motion through the top or bottom and no precipitation or evaporation through the top or sides, (9) can also be written for chimney k as

$$\frac{1}{A_k} \oint_{C_k} \int_0^{p_z^*} (V_n q + V_n Q) \frac{dp^*}{g}\, dC + \overline{P_o}^k - \overline{E}^k = 0 \quad , \tag{10}$$

where $^{-k}$ refers to a horizontal average over an individual convective chimney. We now define the inflow and outflow normal components of air motion separately:

$$V_n^+ = V_n \text{ if } V_n < 0, \text{ else } V_n^+ = 0,$$

$$V_n^- = V_n \text{ if } V_n \geq 0, \text{ else } V_n^- = 0.$$

With this notation (10) becomes

$$\frac{1}{A_k} \oint_{C_k} \int_0^{p_z^*} \left[V_n^+ q_a + V_n^- (q_s + Q)\right] \frac{dp^*}{g}\, dC + \overline{P_o}^k - \overline{E}^k = 0 \quad . \tag{11}$$

The mean inflow specific humidity $\overline{q}^{+k}$ is defined as

$$\overline{q}^{+k} = \frac{\oint_{C_k} \int_0^{p_z^*} V_n^+ \, q_a \, dp^* \, dC}{\oint_{C_k} \int_0^{p_z^*} V_n^+ \, dp^* \, dC} \quad , \tag{12}$$

and the mean outflow specific humidity $\overline{q}^{-k}$ and the mean outflow cloud water $\overline{Q}^{-k}$ as

$$\overline{q}^{-k} = \frac{\oint_{C_k} \int_0^{p_z^*} V_n^- \, q_s \, dp^* \, dC}{\oint_{C_k} \int_0^{p_z^*} V_n^- \, dp^* \, dC} \, , \tag{13}$$

$$\overline{Q}^{-k} = \frac{\oint_{C_k} \int_0^{p_z^*} V_n^- \, Q \, dp^* \, dC}{\oint_{C_k} \int_0^{p_z^*} V_n^- \, dp^* \, dC} \quad . \tag{14}$$

Mass continuity requires that

$$\oint_{C_k} \int_0^{p_z^*} V_n^+ \, dp^* \, dC \equiv - \oint_{C_k} \int_0^{p_z^*} V_n^- \, dp^* \, dC \quad . \tag{15}$$

Let

$$M_k = \frac{1}{g} \oint_{C_k} \int_0^{p_z^*} V_n^- \, dp^* \, dC \ . \tag{16}$$

Combining eqs. (11) through (16) then gives

$$M_k(\overline{q}^{-k} + \overline{Q}^{-k} - \overline{q}^{+k}) + (\overline{P}_o^k - \overline{E}^k) \, A_k = 0 \ , \tag{17}$$

which is simply a restatement of the conservation of moisture in steady state.

If we ignore the evaporation term in comparison with the precipitation term in active precipitating systems, from (17) we then have

$$\overline{P}_o^k \, A_k \approx M_k \, (\overline{q}^{+k} - \overline{q}^{-k} - \overline{Q}^{-k}) \ . \tag{18}$$

For the steady-state tall chimney, by moisture continuity the <u>net</u> moisture transport through the top of the BOMEX volume is identical with the lateral divergence of moisture above; that is,

$$\overline{F}_w^{kT} \, A_k = M_k \, (\overline{q}^{-k} + \overline{Q}^{-k}) \ . \tag{19}$$

Dividing (19) by (18) gives the formula for the moisture flux ratio for steady-state tall convective chimneys:

$$\boxed{\frac{\overline{F}_w^{kT}}{\overline{P}_o^k} = \frac{\overline{q}^{-k} + \overline{Q}^{-k}}{\overline{q}^{+k} - (\overline{q}^{-k} + \overline{Q}^{-k})}} \ . \tag{20}$$

4.2 Steady-State Medium-Size Chimney

Consider a medium-size steady-state convective chimney, in which fraction α of the mass divergence and fraction β of the moisture divergence occur above the volume top, and fractions $1-\alpha$ and $1-\beta$ below the top. For this situation, one can readily show that

$$\boxed{\frac{\overline{F_w}^{kT}}{\overline{P_o}^{k}} = \beta_k \frac{\overline{q}^{-k} + \overline{Q}^{-k}}{\overline{q}^{+k} - (\overline{q}^{-k} + \overline{Q}^{-k})}} \quad . \tag{21}$$

4.3 Growth Stage

To formulate the relationship of precipitation to the other fluxes during the growth stage, it is necessary to average over time. We will assume that rainfall formation effectively begins when the piston (cloud top) reaches the top of the inflow layer. The growth stage continues until the cloud grows to its ultimate level, p_z. Thereafter the steady-state model prevails.

Definitions. Reference pressure levels are (fig. 2):

$p_o^* =$ sea level $\equiv 0$

$p_i^* =$ top of inflow layer

$p_T^* =$ top of BOMEX volume

$p_z^* =$ top of cloud when growth is complete

Reference times are:

$t_i =$ time at which cloud top attains level p_i^*

$t_z =$ time at which cloud top attains level p_z^*

$\Delta t = t_z - t_i$

Notation for averages is:

$\overline{X}^t =$ average X over time interval Δt

$\overline{X}^{a \to b} =$ average X between levels p_a^* and p_b^*

Averaging may be multiple, e.g., $\overline{X}^{t,a \to b}$ is the average both over time and between levels p_a^* and p_b^*.

Moisture flux ratio. The net moisture transport within the cloud chimney through the top of the BOMEX volume during the growth stage is simply the mass of water required to saturate the portion of the cloud chimney above the top surface with water vapor and fill this volume with cloud water. (The pre-existing water vapor in this volume exits laterally.) Expressing this transport as average flux times area times time gives

$$\overline{F_w}^{kTt} A_k \Delta t = A_k \int_{p_T^*}^{p_z^*} \overline{(q_s + Q)}^k \frac{dp^*}{g} = \frac{A_k}{g} (p_z^* - p_T^*) \overline{(q_s + Q)}^{k,T \rightarrow z} . \quad (22)$$

The total rainfall during the growth stage is simply the difference between the mean inflow specific humidity and the saturation specific humidity plus cloud water prevailing at the end of the growth stage, times the mass of air involved; that is,

$$\overline{P_o}^{kt} A_k \Delta t = A_k \int_{p_i^*}^{p_z^*} \left[\overline{q}^{+k} - \overline{(q_s + Q)}^k \right] \frac{dp^*}{g}$$

$$= \frac{A_k}{g} (p_z^* - p_i^*) \left[\overline{q}^{+k} - \overline{(q_s + Q)}^{k,\ i \rightarrow z} \right] \quad (23)$$

where $\overline{q}^{+k}$ is defined in eq. (12). The <u>inflow</u> during the growth stage in the model is steady state, and we can therefore use the steady-state definition. Evaporation has been neglected here as small compared with active precipitation.

By dividing (22) by (23) we obtain the flux/precipitation ratio for the growth stage of cloud chimney k:

$$\boxed{\frac{\overline{F_w}^{kTt} \Delta t}{\overline{P_o}^{kt} \Delta t} = \frac{p_z^* - p_T^*}{p_z^* - p_i^*} \cdot \frac{\overline{q_s + Q}^{k,T \rightarrow z}}{\overline{q}^{+k} - \overline{(q_s + Q)}^{k,i \rightarrow z}}} . \quad (24)$$

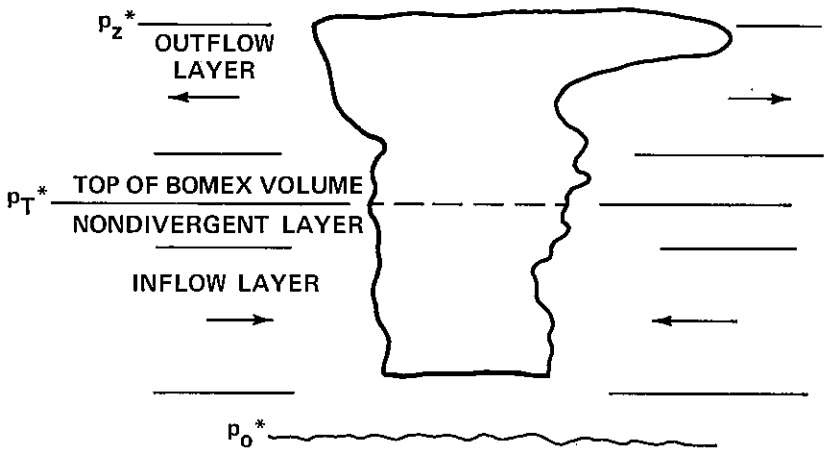

Figure 1.--Cloud chimney model, steady-state tall chimney.

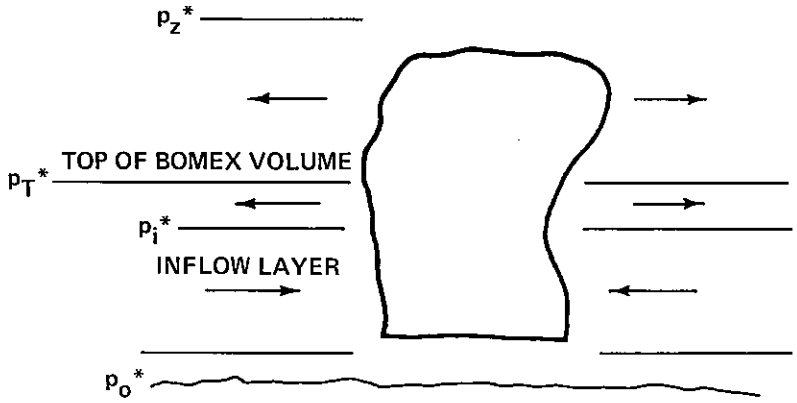

Figure 2.--Cloud chimney model, growth stage.

5. MASS FLUX RATIO

Parameterization of the mass flux in clouds through the top of the BOMEX volume is needed to solve eq. (8). We develop the formulation for the dimensionless ratio in a steady state:

$$\frac{\overline{\omega^*}^{kT}}{g} \frac{\overline{q}^{+k}}{\overline{p_o}^{k}} .$$

Continuity of mass in the steady state requires for a tall cloud chimney that

$$M_k = \frac{\overline{\omega^*}^{kT}}{g} A_k , \tag{25}$$

where M_k is the mass transport defined by eq. (16).

From (18) and (19),

$$M_k \approx A_k \frac{\overline{P_o}^{k} + \overline{F_w}^{kT}}{\overline{q}^{+k}} , \tag{26}$$

so that

$$\frac{\overline{\omega^*}^{kT}}{g} = \frac{\overline{P_o}^{k} + \overline{F_w}^{kT}}{\overline{q}^{+k}} . \tag{27}$$

For the cloudy area as a whole, if tall chimneys predominate, summing (27) over cloud chimneys gives

$$\frac{\overline{\omega^* cT}}{g} = \frac{1}{A_c} \sum_{k=1}^{n} \frac{\overline{P_o}^k + \overline{F_w}^{kT}}{\overline{q}^{+k}} A_k \ . \tag{28}$$

If it is assumed that the percentage variation of $\overline{q}^{+k}$, the average inflow specific humidity in BOMEX precipitating clouds, was small compared with the variation of precipitation and upward moisture flux from one convective chimney to another, i.e.,

$$\frac{\overline{P_o}^k + \overline{F_w}^{kT}}{\overline{q}^{+k}} \approx \frac{\overline{P_o}^k + \overline{F_w}^{kT}}{\overline{q}^{+c}} \ , \tag{29}$$

then

$$\frac{\overline{\omega^* cT}}{g} \approx \frac{\overline{P_o}^c + \overline{F_w}^{cT}}{\overline{q}^{+c}} = \frac{\overline{P_o}^c}{\overline{q}^{+c}} \left[1 + \frac{\overline{F_w}^{cT}}{\overline{P_o}^c} \right] . \tag{30}$$

To start with the average rain, $\overline{P_o}^B$, instead of the cloudy area average, $\overline{P_o}^c$, over the BOMEX square, we use the identity

$$\overline{P_o}^c \equiv \frac{A_B}{A_c} \overline{P_o}^B \tag{31}$$

in (30), and obtain

$$\boxed{\frac{\overline{\omega^*}^{cT}}{g}\,\frac{A_c}{A_B} = \frac{\overline{P_o}^{B}}{\overline{q}^{+c}}\left[1 + \frac{\overline{F_w}^{cT}}{\overline{P_o}^{c}}\right]} \quad , \tag{32}$$

which provides the term to substitute in eq. (8) based on tall chimneys. This term also appears later in eq. (44).

Now consider medium chimneys. Equation (25) becomes

$$\alpha_k\, M_k = \frac{\overline{\omega^*}^{kT}}{g}\, A_k \ , \tag{25a}$$

where α, as previously defined, is the fraction of the mass divergence above the top of the BOMEX volume. Using (21) instead of (20) and proceeding as before leads to

$$\frac{\overline{\omega^*}^{kT}}{g}\,\frac{\overline{q}^{+k}}{\overline{P_o}^{k}} = \alpha_k\left(\beta_k + \frac{\overline{F_w}^{kT}}{\overline{P_o}^{k}}\right), \tag{28a}$$

which shows the natural result that there is less mass transport through the top per unit rain for medium chimneys than for tall ones. Lacking knowledge of α and β, we feel justified in using eq. (32) on the grounds that most of the total volume of rain is from tall clouds.

6. ENTHALPY FLUX

The steady-state enthalpy flux through the top of the BOMEX volume,

$$\overline{F_H}^{BT} = \frac{\overline{\omega^* c_p T}^{BT}}{g} \ , \tag{33}$$

can be partitioned into cloud and clear-air portions, in accordance with eq. (1):

$$\overline{F_H}^{BT} = \frac{A_c}{A_B} \overline{F_H}^{cT} + \left(1 - \frac{A_c}{A_B} \right) \overline{F_H}^{aT} \quad . \tag{34}$$

6.1 Clear-Air Flux

The clear-air flux through the top of the volume is

$$\overline{F_H}^{aT} = \frac{c_p}{g} \left[\overline{\omega^*}^{aT} \overline{T}^{aT} + (\omega^*)^{aT} (T)^{aT} \right] \quad . \tag{35}$$

We will neglect the clear-air covariance term of necessity in the hope that it is small, the same as the moisture clear-air covariance term (sec. 2); that is,

$$\overline{F_H}^{aT} \approx \frac{\overline{\omega^*}^{aT}}{g} c_p \overline{T}^{aT} \quad . \tag{36}$$

6.2 Cloud Flux

The cloud flux is

$$\overline{F_H}^{cT} = \frac{1}{A_c} \sum_{k=1}^{n} A_k \overline{\frac{\omega^*}{g} c_p T}^{kT} \quad . \tag{37}$$

We express cloud temperatures as departures from the mean ambient clear-air temperature on the same p* surface. Further, to facilitate keeping track of approximations in handling the cloud covariance term, we define an <u>effective</u> mean temperature departure, $\Delta T'_k$, for each cloud chimney as

$$\Delta T'_{kT} = \frac{\overline{\omega^* T}^{kT}}{\overline{\omega^*}^{kT}} - \overline{T}^{aT} \quad . \tag{38}$$

Rearranging, we have

$$\overline{\omega^* T}^{kT} = \overline{\omega^*}^{kT} \left(\overline{T}^{aT} + \Delta T'_{kT} \right) \quad , \tag{39}$$

and substituting in (37) gives

$$\overline{F_H}^{cT} = \frac{1}{A_c} \sum_{k=1}^{n} A_k \frac{\overline{\omega^*}^{kT}}{g} c_p \left(\overline{T}^{aT} + \Delta T'_{kT} \right) \quad . \tag{40}$$

Similarly, we can define an effective mean cloud temperature departure, pertaining to all clouds collectively, as

$$\Delta T'_{cT} = \frac{\overline{\omega^* T}^{cT}}{\overline{\omega^*}^{cT}} - \overline{T}^{aT} \quad , \tag{41}$$

which leads to

$$\overline{F_H}^{cT} = \frac{\overline{\omega^*}^{cT}}{g} c_p \left(\overline{T}^{aT} + \Delta T'_{cT} \right) \quad . \tag{42}$$

Whether one uses (40) or (42) depends on whether $\Delta T'$ can be parameterized for individual cloud chimneys. We will proceed here with the overall $\Delta T'$ and use (42). Corresponding analysis with (40) and individual values of cloud chimney $\Delta T'$s can be readily developed if sufficient cloud temperature information can be adduced to justify it.

6.3 Total Flux

Combining (34), (36), and (42) gives the following expression for the total enthalpy flux through the top of the BOMEX volume:

$$\overline{F_H}^{BT} = \frac{A_c}{A_B} \frac{\overline{\omega^*}^{cT}}{g} c_p \left(\overline{T}^{aT} + \Delta T'_{cT} \right) + \left(1 - \frac{A_c}{A_B}\right) \frac{\overline{\omega^*}^{aT}}{g} c_p \overline{T}^{aT} \quad . \tag{43}$$

Substitution of

$$\left(1 - \frac{A_c}{A_B}\right) \frac{\overline{\omega^*}^{aT}}{g} = \frac{\overline{\omega^*}^{BT}}{g} - \frac{A_c}{A_B} \frac{\overline{\omega^*}^{cT}}{g} \tag{8a}$$

from (8) in (43) gives

$$\boxed{\overline{F_H}^{BT} = \frac{\overline{\omega^*}^{BT}}{g} c_p \overline{T}^{aT} + \frac{A_c}{A_B} \frac{\overline{\omega^*}^{cT}}{g} c_p \Delta T'_{cT}} \quad . \tag{44}$$

The important fact emerging from the last term of (44) is that the difference between the cloud and environment temperatures, not the absolute cloud temperature, is the parameter needed to estimate the cloud contribution to enthalpy flux. To estimate enthalpy flux from (44), the individual terms are evaluated as follows:

(a) $\overline{\omega^*}^{BT}$ from the overall mass budget (Holland and Rasmusson, 1973).

(b) $\overline{T}^{aT}$ averaged from radiosonde observations.

(c) A_c from the parameterized clouds,

$$A_c = \sum_{k=1}^{n} A_k \quad . \tag{45}$$

(d) $\frac{\overline{\omega^*}^{cT}}{g}$ from the parameterized moisture flux and precipitation in eq. (28) or (32).

(e) $\Delta T'_{cT}$, for which there were no measurements in BOMEX, is parameterized via considerations relating buoyancy and potential pseudo-wet-bulb temperature as described in the next section.

In (d) above it is assumed that steady-state tall chimneys predominate. This gives an overestimate of $\overline{\omega^*}^{ct}/g$ to the extent that medium-size steady-state chimneys and the growth stage contribute to the rainfall. Equation (28a) is a discount formula for the medium chimneys. A similar formula could be developed for the growth stage. For disturbed weather during BOMEX these adjustments are small compared with the uncertainty in $\Delta T'_{cT}$ and therefore do not appear warranted.

7. CLOUD PARAMETERS

In solving a geophysical problem by a parameterization method, relevant geophysical variables are assigned values believed to be representative of conditions the problem treats. The assigned values are derived from a combination of observation and experience. This section covers the assignment of basic values to cloud parameters, the clouds of interest being those that produced rain from within the BOMEX volume. The cloud environment affects the clouds and thus also requires parameterization.

7.1 Representative Environmental Clear-Air Sounding

The temperature and specific humidity of the lower levels are entrained into the cloud and determine its characteristics. The environmental air density at middle levels exercises stringent control on cloud growth via buoyancy. Here we specify the temperatures and specific humidities, as functions of pressure, intended to be characteristic of the immediate environment of those cloud chimneys actively producing rain.

The immediate environment of active cloud chimneys differs from overall average BOMEX conditions. An overall average radiosonde sounding exhibits too great a stability to permit active deep convection, which is not surprising since fair weather was the prevailing regime during most of BOMEX. The trade inversion disappears when it rains substantially. The cloud chimney environment is therefore modeled on a very few soundings taken during periods of greatest weather disturbance.

Temperature and Humidity Below 400 mb. Most weather disturbances passed across the southern part of the BOMEX square array, affecting the Discoverer at the southeast corner and the Mt. Mitchell at the southwest corner. The following radiosonde soundings were identified as being taken when rain was falling at the ship or when showers were in sight:

Discoverer	Mt. Mitchell
2231 GMT, June 28, 1969	1924 GMT, June 23 1969
0301 GMT, June 29, 1969	1155 GMT, June 25, 1969
0602 GMT, June 29, 1969	1945 GMT, June 28, 1969
0430 GMT, July 1, 1969	1154 GMT, June 29, 1969

A mean was taken of the Discoverer soundings (fig. 3, right panel). Relative humidities were corrected for temperature lag of the radiosonde hygristor (Sanders et al., 1973) before derivation of the specific humidity, q, and dewpoint, T_d. (The lag correction increases the wet-bulb temperature by about 0.75° at lower levels, which is sufficient to materially influence the buoyancy of clouds growing from this air.) Sanders et al. (1973) also describe a radiation correction to daytime radiosondes, but this correction did not have to be applied to the Discoverer soundings, which were taken at night.

The humidities shown by the mean sounding in figure 3 suggest that above about 800 mb the radiosondes were indeed rising through clear or partly cloudy air and not through a deep altostratus or cumulonimbus cloud, although rain was observed at or near the ship. This sounding is therefore adopted as the environment of all cloud chimneys discussed in this paper.

As a check, the temperature mean for the four Mt. Mitchell soundings was also computed (fig. 4) and found to be quite similar to the Discoverer mean. The humidities from the Mt. Mitchell soundings were ignored, being daytime measurements affected by insolation error. Calculations, in which the Sanders et al. correction was incorporated, showed that this daytime measurement error depressed calculated low-level wet-bulb temperatures sufficiently to prohibit their use in the model. No suitable nighttime soundings from the Mt. Mitchell during disturbed weather were available.

Potential Wet-Bulb Temperature. The potential wet-bulb temperature was calculated from the mean adopted environmental sounding graphically on a pseudo-adiabatic chart by the standard scheme illustrated in figure 5. We symbolize potential pseudo-wet-bulb temperature by "τ" instead of the conventional "θ_{sw}" to minimize multiple subscripts, and τ_e thus derived is shown in the left panel of figure 3.

Another quantity needed is the environmental saturation potential wet-bulb temperature. This we symbolize by "τ_{se}" and define as the potential wet-bulb temperature that would prevail if the air were saturated at its existing temperature and pressure. This value is readily obtained from a pseudo-adiabatic chart by reading the label on the saturation adiabat passing through the desired temperature-vs.-pressure point. The environmental τ_{se} obtained in this way is also shown in the left panel of figure 3.

Temperature Above 400 mb. Figure 3 is based on soundings that terminated at 400 mb. To provide the needed view of the prevailing upper tropospheric temperatures, temperatures at higher levels were averaged from Discoverer soundings on June 27, 2318 GMT, and June 30, 0003 GMT. The entire curve above 400 mb was then shifted 0.4°C to make the trace continuous at 400 mb. These adjusted upper temperatures are shown in figure 6.

7.2 Cloud Temperature

Cloud temperature is parameterized not from observations, since no BOMEX soundings were detected to have remained in convective clouds through great depth, but by dynamic considerations in relation to the representative environmental sounding depicted in figures 3 and 6.

It is assumed that:

(a) The cloud is slightly buoyant; that is, its density is not greater than that of the environment at the same pressure at any level and is less than that of the environment at some levels.

(b) The cloud is saturated.

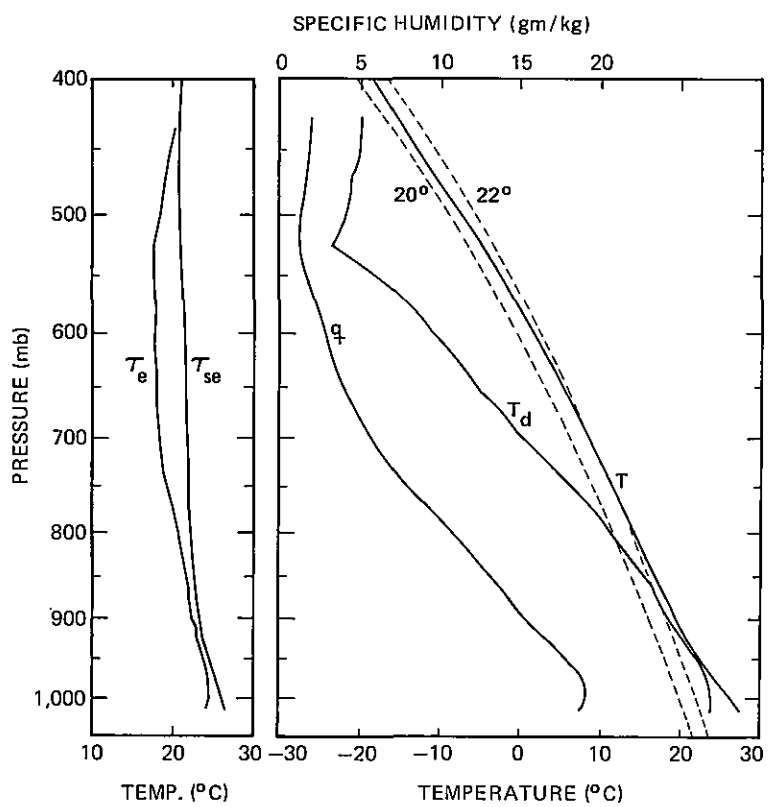

Figure 3.--Model environmental temperature and humidity, based on selected Discoverer *soundings. T = temperature, T_d = dew-point, q = specific humidity, τ_e = potential wet-bulb temperature, and τ_{se} = saturation potential wet-bulb temperature.*

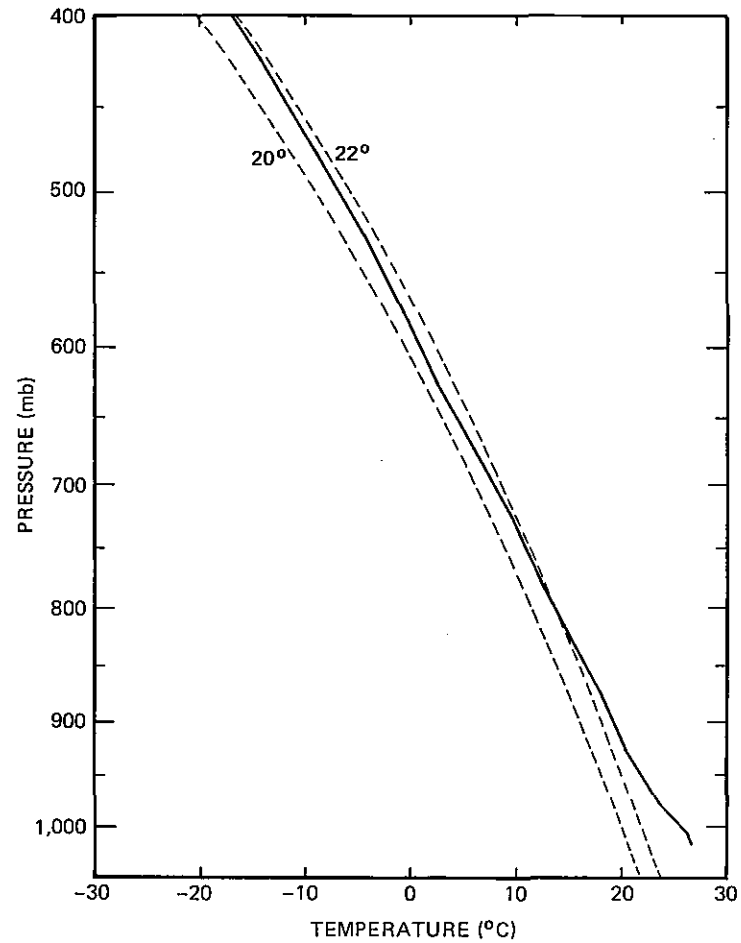

Figure 4.--Mean environmental temperature sounding, Mt. Mitchell.

(c) The relative density difference between cloud and environment can be replaced[1] by the relative temperature difference, $\Delta T/T$.

(d) The cloud potential pseudo-wet-bulb temperature, τ_c, is constant throughout the nondivergent and outflow layers.

(e) The potential pseudo-wet-bulb temperature, τ, is a conservative property in the inflow layer. Thus τ_c at any cloud level is equal to the average environmental τ_e below that level, weighted by mass inflow rate.

From assumptions (b) and (c) and the definition of environmental saturation potential pseudo-wet-bulb temperature, τ_{se}, previously given, the temperature difference ΔT between the cloud and its environment,

$$\Delta T = T_c - T_e \quad , \tag{46a}$$

is very closely approximated by

$$\Delta T \approx \tau_c - \tau_{se} \quad , \tag{46b}$$

where all quantities are at the same pressure.

Figures 3 and 6 show that the model environment is characterized by a deep layer from about 700 mb to 200 mb in which τ_{se} remains in the narrow range of 20.8°C to 22°C. If, as assumed under (a) above, the cloud is to be slightly buoyant, i.e., ΔT is small, then clearly the constant τ_c characterizing the middle and upper parts of the cloud must lie within this range. Outside this range on the cold side would not provide buoyancy, while outside this range on the warm side would provide more than slight buoyancy.

We now apply conservation of τ, assumption (e), for further guidance in parameterizing τ_c. By inspecting the τ_e curve in figure 3 one can readily devise entrainment weights to yield a mean weighted inflow $\overline{\tau_e}^+$ of 22°C. One can also devise weights yielding 21°C, but this seems less probable and requires entrainment to about 700 mb. We adopt 22°C for the basic parametric mean inflow, which must be identical for τ_e and middle and upper τ_c. To illustrate the process, one set of inflow weights that would yield a mean inflow $\overline{\tau_e}^+$ of 22°C is shown in figure 7, where the bottom layer includes inflow through the cloud base.

---

[1]The liquid water load increases cloud density relative to the environment on the order of 0.1 percent. But higher water vapor concentration (virtual temperature difference) decreases cloud density relative to the environment. This is about 0.1 percent at 500 mb in figure 3. These opposite effects are neglected.

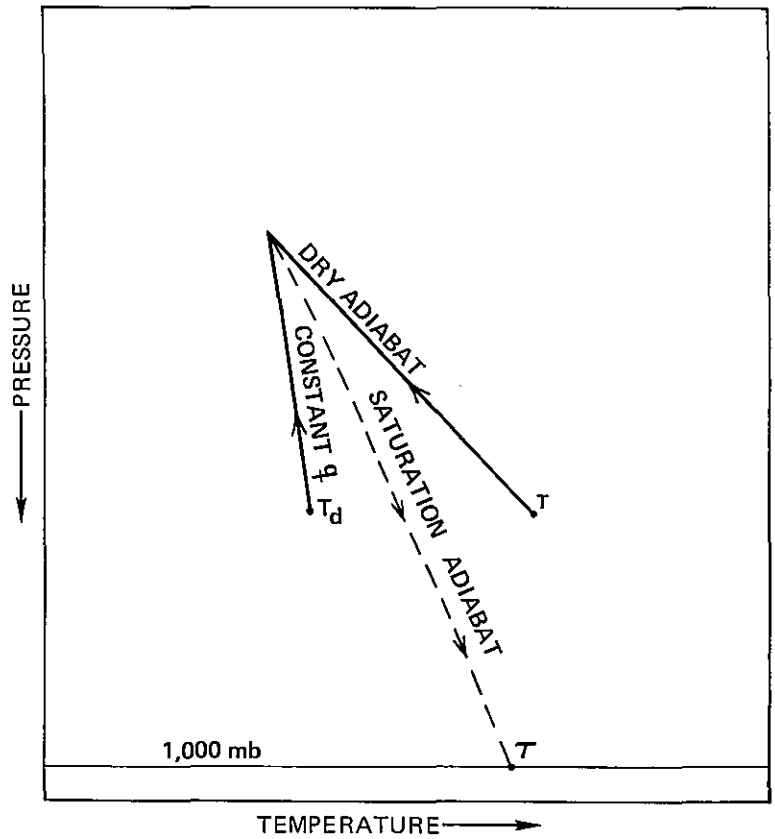

Figure 5.--Schematic illustration of graphical determination of potential wet-bulb temperature, τ, from temperature, T, and dewpoint, T_d.

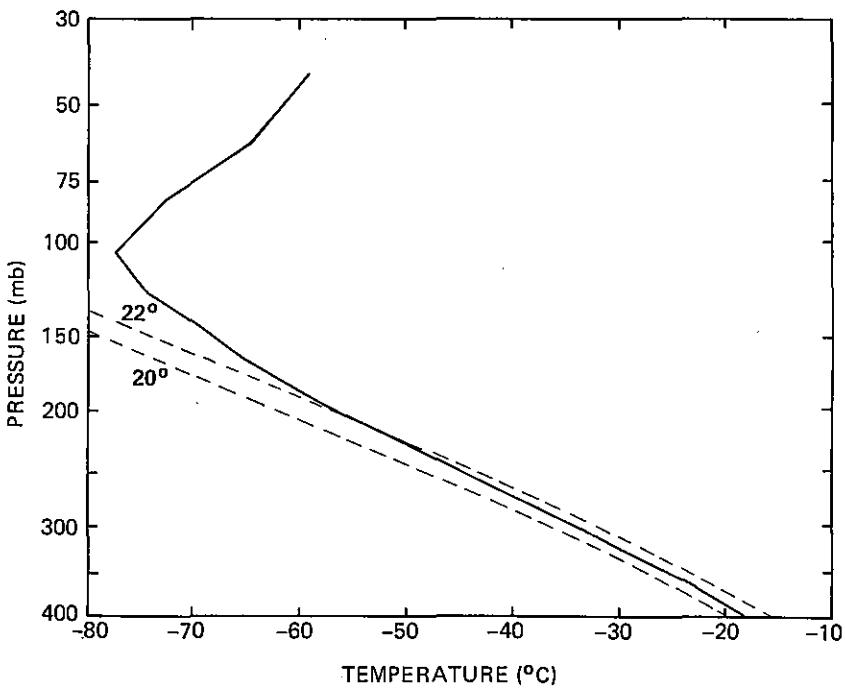

Figure 6.--Extension of environmental temperature of figure 3 to upper levels.

7.3 Mean Inflow Specific Humidity, $\overline{q}^{+}$

The mean inflow specific humidity for the layers and weights shown in figure 7 is 14.0 gm/kg.

7.4 Cloud Water, Q

Cloud water concentration, whether liquid or frozen, is required to evaluate the exit of water substance from the cloud chimney in the divergent layer, e.g., eq. (20). Many measurements have been made of cloud water concentrations on flights through cumulus clouds but only a few at cumulonimbus outflow levels. For guidance on this we turn to the work by Ackerman (1963). She reports on liquid water measurements within the cloud bands of four hurricanes, at elevations up to 18,000 ft. What she calls "convective type measurements" are in most cases coincident with radar echoes, as shown by figure 2 in her paper. Our table 1 is abstracted from her tables 1 and 2, which are based on liquid water measurements only (the system did not respond to ice), but she did not think this was a significant omission at the prevailing temperature range (down to $-6^{o}C$).

We can only surmise that the more vigorous BOMEX convective chimneys were somewhat like ordinary hurricanes with regard to cloud water concentration, but that a few strong hurricanes would be wetter. We view Daisy on August 27, 1958, as this more vigorous breed and the other hurricanes in table 1 as average. Concentrating on the three upper level flights in table 1 we choose 0.75 gm/m^3 as the basic outflow $\overline{Q}^{-}$ for BOMEX.

7.5 Pressure at Top of BOMEX Volume

As noted earlier, the top of the BOMEX volume is at $p^* = 500$ mb. The mean sea-level pressure on the adopted environmental sounding, based on the Discoverer rainy-day soundings, is 1,014 mb. We assign 514 as the pressure at the top of the volume for parameterization calculations.

7.6 Height Vs. Pressure

In the next step, evaluating $\overline{q}^{-}$, pressure is more convenient to use than height as a vertical coordinate. A pressure-height relation is derived by applying standard aerological tables (List, 1951) to the $\tau = 22^{o}C$ pseudo-adiabat. This is shown in table 2 and graphically presented in figure 8.

7.7 Mean Outflow Specific Humidity, $\overline{q}^{-}$

At what levels relative to the cloud top is the outflow from the steady-state cloud chimney? Considering a cumulonimbus with a distinct anvil top, we make the pure assumptions that:

Table 1.--Convective cloud liquid water measurements in hurricanes (after Ackerman, 1963)

Hurricane	Date	Flight level (ft)	Temp. range (°C)	No. of observations	Liquid water (gm/m^3)		
					Median	Upper quartile	Maximum
				Upper levels			
Carrie	9/15/57	18,000	+2 to -3	264	0.52	0.70	2.40
Becky	8/13/58	15,600	+2 to -4	597	0.65	0.82	2.27
Daisy	8/25/58	15,600	+6 to -3	1805	0.58	0.79	3.60
				Lower levels			
Daisy	8/27/58	13,000	+3 to +7	547	1.60	3.28	9.51
Helene	9/24/58	13,000	+1 to +7	983	0.65	0.96	7.68
Helene	9/24/58	9,000	+9 to +13	81	0.72	1.03	2.70

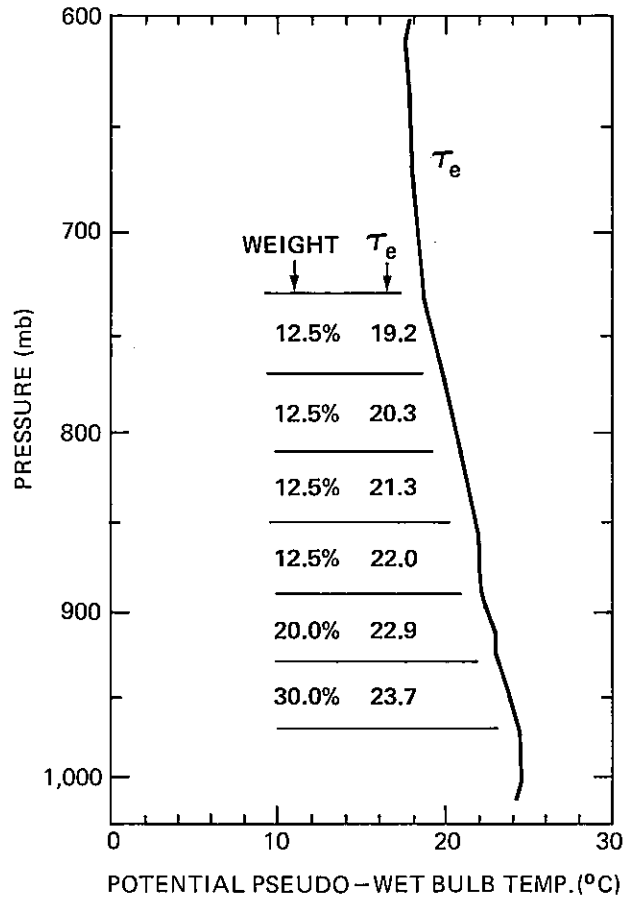

Figure 7.--Weights and mean potential wet-bulb temperature, τ_e, of sublayers of inflow layer; τ_e curve same as in fig.3.

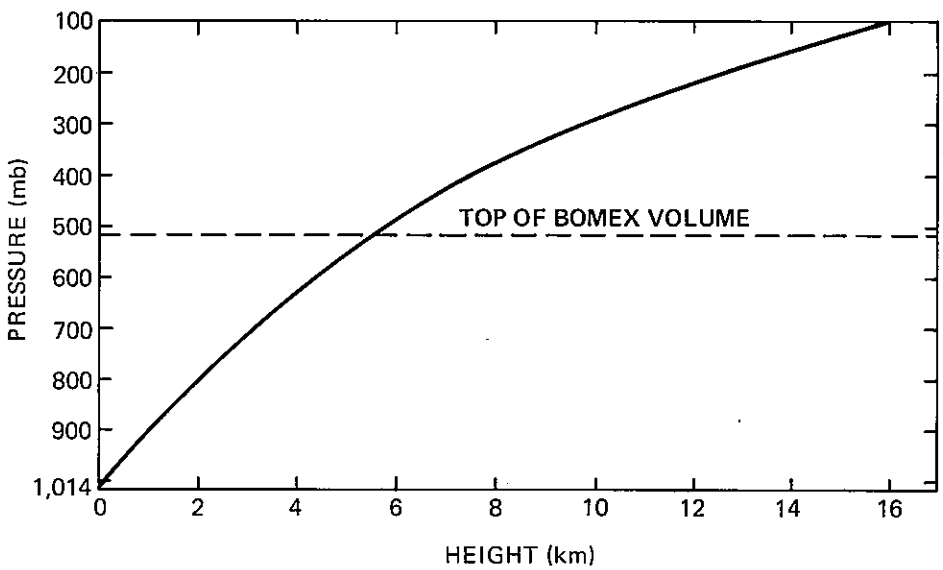

Figure 8.--Pressure-height relationship in atmosphere with τ = 22°C.

(a) The upper 20 percent of the cloud mass constitutes the outflow layer. For this calculation we place the cloud base at 960 mb.

(b) Uniform divergence with height prevails within this outflow layer.

With these assumptions, $\bar{q}^{-}$ is identical to the mean q_s on the $\tau = 22^{o}C$ pseudo-adiabat between two pressure levels. These mean outflow $\bar{q}^{-}$'s are listed in table 3 and graphically shown in figure 9 for a range of cloud heights. For clouds of medium height not all the moist outflow is above the top of the BOMEX volume. The fraction that is, β, is needed for later calculation and is also shown in the table and on the graph.

Table 2.--Height vs. pressure in pseudo-adiabatic atmosphere (τ_s = 22°C)

Height (m)	Pressure (mb)
0	1,014
121	1,000
1,034	900
2,040	800
3,160	700
4,424	600
5,880	500
7,597	400
9,697	300
12,414	200
14,163	150
16,397	100

7.8 Cloud Height

Cloud height requires special treatment and is discussed in section 8.

7.9 Influence of Cloud Parameters on Moisture Flux Ratio

In this section we make some simple tests of the sensitivity of the moisture flux ratio to values of the several cloud parameters. Table 4 illustrates the moisture flux ratio, computed by eq. (21), for a steady-state cloud with top at 300 mb, varying one constituent parameter at a time. Line 1 under "assigned parameters" shows the basic values assigned. On each succeeding line one parameter value is changed, indicated by underlining.

*Table 3.--Moisture outflow values for basic parameterization**

Cloud height, p_z (mb)	Base of outflow layer, p_b (mb)	Mean outflow specific humidity, $\overline{q}$ (gm/kg)	Fraction of moist outflow above top of volume, β
100	272	0.09	1.0
150	312	0.31	1.0
200	352	0.66	1.0
250	392	1.24	1.0
300	432	2.00	1.0
350	472	2.92	1.0
400	512	3.99	1.0
402	514	4.01	1.0
425	532	4.56	0.72
450	552	5.10	0.57
500	592	6.25	0.13
514	603	6.58	0

*Cloud base at 960 mb; uniform divergence from upper 20 percent of cloud; τ = 22°C; top of BOMEX volume at 514 mb.

Table 4.--Comparative parameters for steady-state cloud with base at 960 mb (486 m) and summit at 300 mb (9,697 m)

Line	Assigned parameters									Resulting parameters				
	τ (°C)	$\bar{q}^+$ (gm/kg)	D	W*					Q (gm/kg)	$\bar{q}^-$	$\bar{q}^+ - (\bar{q}^- + Q)$	Ratio to line 1	$\frac{\bar{F}_w kT}{\bar{P}_o k}$	Ratio to line 1
				1	2	3	4	5						
1	22	14	0.2	0.2	0.2	0.2	0.2	0.2	0.75	2.00	11.25	1.00	0.244	1.00
2	21	13.1	0.2	0.2	0.2	0.2	0.2	0.2	0.75	1.70	10.65	0.95	0.230	0.94
3	22	12.6	0.2	0.2	0.2	0.2	0.2	0.2	0.75	2.00	9.85	0.88	0.279	1.14
4	22	14	0.3	0.2	0.2	0.2	0.2	0.2	0.75	2.74	10.51	0.93	0.332	1.36
5	22	14	0.2	0.1	0.15	0.2	0.25	0.3	0.75	1.79	12.39	1.10	0.221	0.905
6	22	14	0.2	0.3	0.25	0.2	0.15	0.1	0.75	2.33	10.92	0.97	0.282	1.16
7	22	14	0.2	0.2	0.2	0.2	0.2	0.2	1.00	2.00	11.00	0.98	0.272	1.11

*Divide divergence layer into five equal sublayers. The W's give fraction of mass divergence in each sublayer, from lowest (1) to highest (5).

The parameter D is the fraction of the cloud depth that comprises the outflow layer. The W's define the divergence profile within the outflow layer as explained in the footnote to the table. The quantity $\overline{q}^{+} - (\overline{q}^{-} + Q)$ is listed as an indicator of the comparative rain intensity; see eq. (18).

Temperature. Reducing the cloud τ by $1^{\circ}C$ and changing the environment to maintain the same buoyancy reduces the rain by 5 percent and the flux ratio by 6 percent (table 4, line 2).

Inflow. Reducing the inflow $\overline{q}^{+}$ but holding cloud τ constant, which is done by bringing in the inflow at higher levels, reduces the rain and increases the flux ratio (table 4, line 3). The cloud is made less efficient as a rain producer.

Depth of Divergence Layer. Increasing the depth of the divergence layer by 50 percent, from 0.2 to 0.3, permitting the escape of water vapor at lower and warmer elevations, substantially increases the flux ratio (table 4, line 4). Varying D in this way would change the moisture flux ratio less for clouds not as tall as those covered in table 4, because β would vary; see eq. (21). For both values of D, $\beta = 1.0$ for the 300-mb cloud.

Divergence Profile. Shifting the divergence to higher and colder elevations (table 4, line 5) increases the efficiency of rain production and decreases the net flux ratio, and conversely (line 6).

Liquid Water. A substantial increase in Q of 33 percent produces a moderate increase in the flux ratio of 11 percent (table 4, line 7).

Growth Stage. Changes like the ones on lines 2, 3, and 7 would produce the same kinds of effects on the rain and moisture flux during the growth stage. Lines 4, 5, and 6 do not apply.

Summary. The efficiency of the cloud and the resulting moisture flux ratio is most sensitive to the pressure at which processes occur, which is not surprising for a thermodynamic system like the one discussed here. The magnitudes of τ and Q (table 4, lines 2 and 7) are not dependent on pressure. Fairly severe variations in these quantities produce only moderate variations in the flux ratio, ~ 10 percent. The other factors are dependent on pressure and are more influential.

8. CLOUD HEIGHT EFFECTS: APPLICATION OF RADAR DATA

8.1 Moisture Flux Ratio vs. Cloud Height

The ratio of moisture flux through the top of the BOMEX volume to rainfall rate for steady-state clouds as calculated from eq. (21) is shown in table 5 and figure 10 for the basic parameterization indicated in the table. The cusp in the curve denotes the boundary between medium and tall clouds. The taller the cloud, the more efficient it is as rain producer (smaller flux ratio), but below the cusp, part of the water-vapor escape is within the BOMEX volume and does not appear in the computed flux ratio.

*Table 5.--Steady-state moisture flux ratio from eq. (21) for basic parameterization**

Cloud height, p_z (mb)	Base of outflow layer, p_b (mb)	Mean outflow specific humidity, $\bar{q}^-$ (g/kg)	$\bar{q}^- + Q$ (gm/kg)	Fraction of outflow above top, β	Moisture flux ratio, $\bar{F}_w kT/\bar{P}_o k$
100	272	0.09	0.84	1.0	0.063
150	312	0.31	1.06	1.0	0.082
200	352	0.66	1.41	1.0	0.112
250	392	1.24	1.99	1.0	0.166
300	432	2.00	2.75	1.0	0.244
350	472	2.92	3.67	1.0	0.355
400	512	3.99	4.74	1.0	0.512
402	514	4.01	4.76	1.0	0.515
425	532	4.56	5.31	0.79	0.48
450	552	5.10	5.85	0.57	0.41
500	592	6.25	7.00	0.13	0.13
514	603	6.58	7.33	0	0

*T_p = 514 mb; $\bar{q}^+$ = 14.0 gm/kg; Q = 0.75 gm/kg; τ = 22°C; cloud base at 960 mb; uniform divergence in upper 20 percent of cloud.

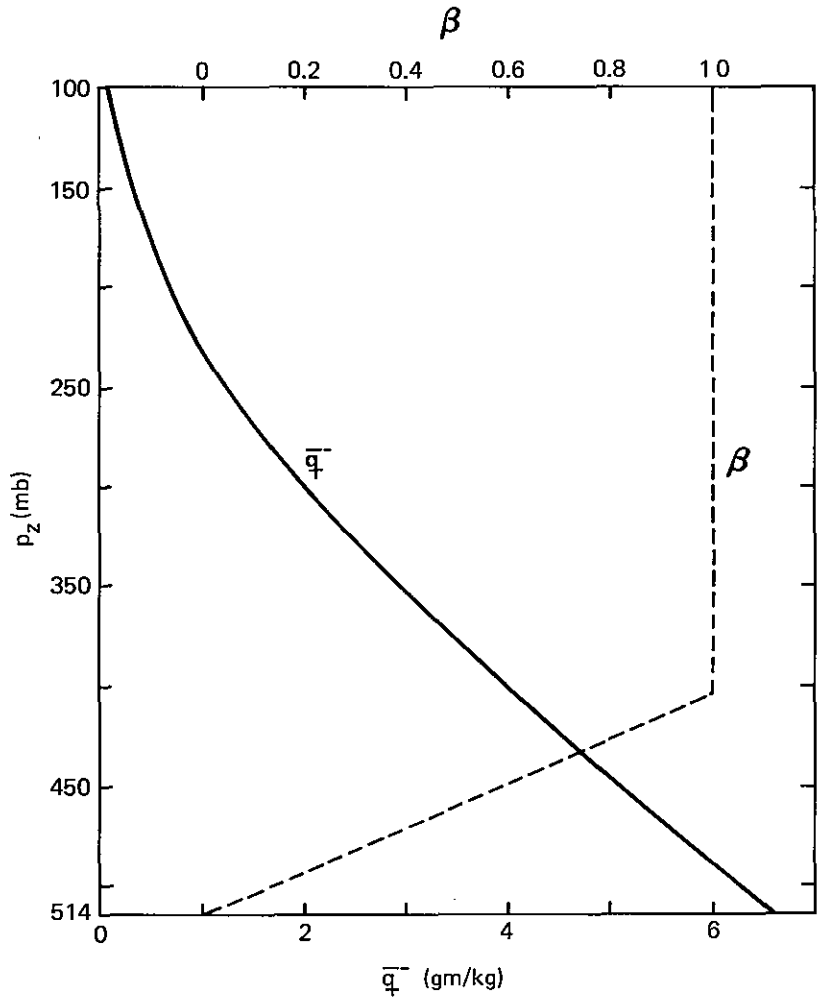

Figure 9.--Mean outflow specific humidity, $\bar{q}^-$, vs. cloud chimney height. Basic parameterization. β = fraction of outflow above BOMEX volume top.

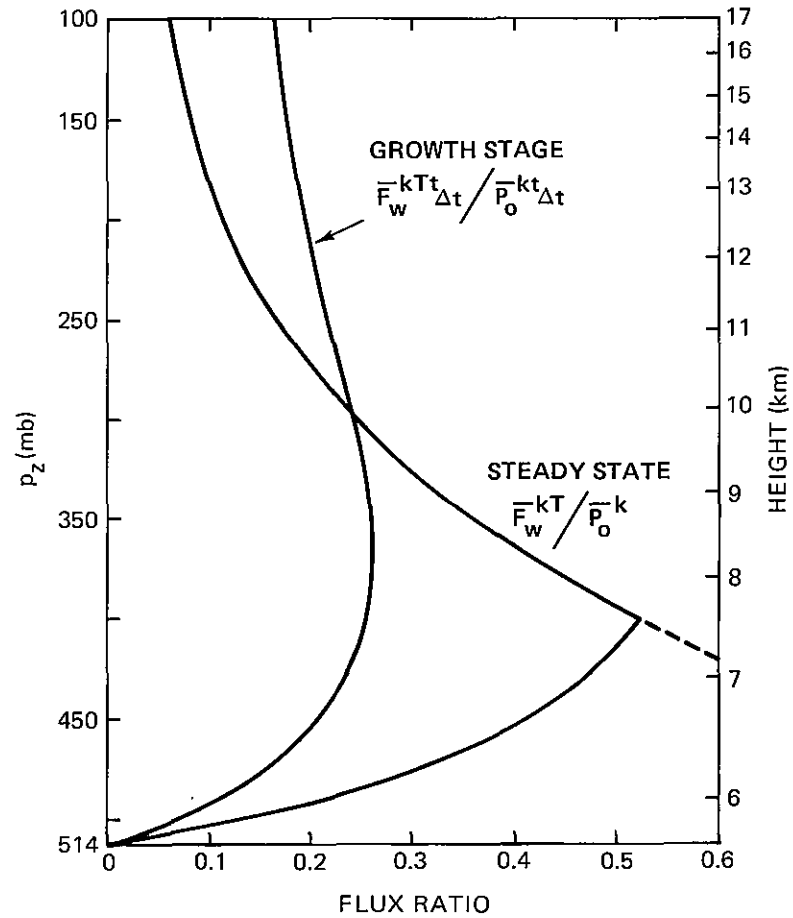

Figure 10.--Net moisture flux ratio at BOMEX volume top vs. cloud chimney height. Basic parameterization.

The corresponding growth-stage moisture flux ratio is computed in table 6 and graphically shown in figure 10. This is the ratio of the total flux during the growth stage to the total rain production. It is evident from the figure that the moisture flux ratio is highly dependent on cloud height in a nonlinear way. Experience suggests that cloud height is not a unique function of rainfall rate. Thus, to parameterize the moisture flux for a given rainfall rate, we need to presume an ensemble of clouds of different heights. If we take care of cloud height in this way, then we are justified in using the single basic values of the other parameters proposed in section 7. For information on cloud heights we turn to the work by Hudlow (1971).

8.2 Cloud Height Vs. Rainfall Rate From Radar

The BOMEX radar program included sequential tilted antenna scans with "gain-stepping" of the power return from the radar on Barbados (Hudlow, 1970). Thus concurrent information is available on maximum power return, PR, and echo height. Hudlow selected 48 such paired values to represent the BOMEX population of echoes. These are plotted in figure 11. The power return values are range normalized to a range of 50 nmi. The reader is referred to Hudlow (1971) for this and other details of the radar observations and data reduction. The curve fitting in figure 11 is explained below.

Hudlow (1971) also derived a statistical relationship of rainfall rate to power return by compositing theory, data, and climatology of drop sizes (the last from other areas; no observations were made during BOMEX). From the statistical relationship, an average rainfall rate over each echo area is obtained. Combining these analyses leads to the graph in figure 12, showing maximum power return vs. echo average rainfall. Based on this relationship, the abscissa scale in figure 11 was converted to echo average rainfall rate. By definition, the cloud chimneys under discussion here are coincident with radar echoes.

The curves in figure 11 show the probability distribution of cloud heights for a given power return (or rainfall rate) based on the 48 cases. To facilitate the analysis of these data, each variable was converted to a normal distribution by a log transformation. Tests for skewness and kurtosis verified that the transformed variables were indeed normal. A regression line was fitted to the normalized variables, and confidence bands were placed about it. These variables were then converted back to the original frame and plotted in the figure along with the original data. The 50-percent line is the transformed regression line, and the other lines enclose the respective confidence bands. The curves are labeled as percentage of cloud heights, from low to high, for a given power return.

8.3 Moisture Flux Ratio Vs. Rainfall Rate

The parameterization of the moisture flux ratio vs. rainfall rate for an echo in the steady state can now be completed through the following steps:

(1) Reading the expected cloud heights at the curves in figure 11 which represent the midpoints of the quintiles for the echo mean rainfall rate.

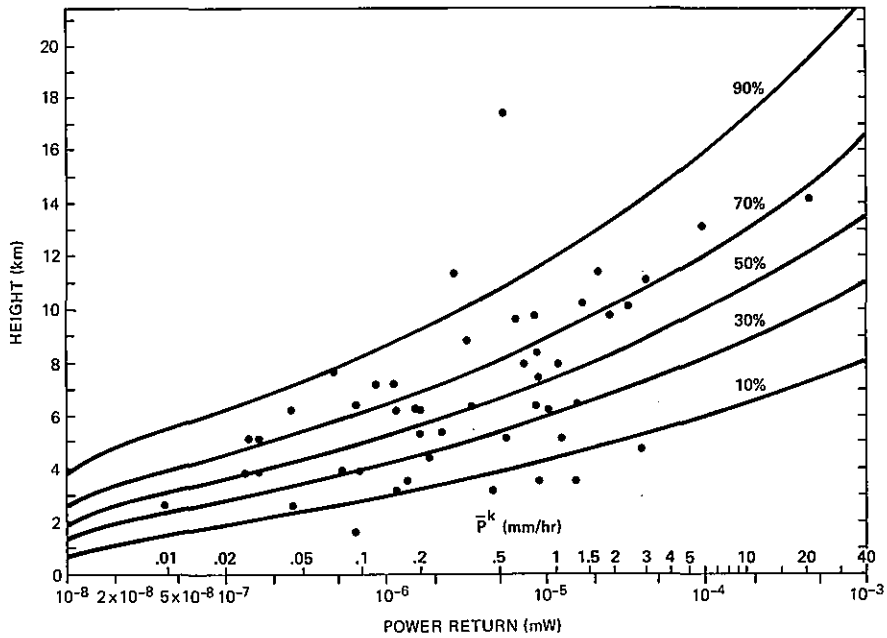

Figure 11.--Echo summit height vs. radar maximum power return and mean echo rainfall rate, selected BOMEX radar echoes.

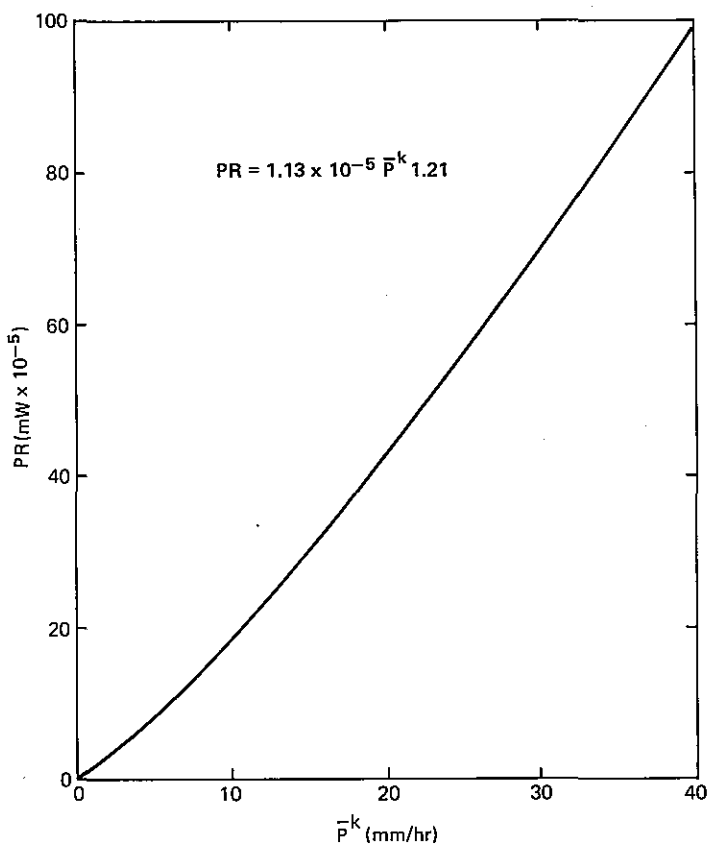

Figure 12.--Radar echo maximum power return, PR, vs. mean echo rainfall rate, $\bar{P}^k_o$. (Hudlow, 1971).

Table 6.--Growth stage moisture flux ratio from eq (24) for basic parameterization[1]

Cloud height, p_z (mb)	$\frac{(P_T^* - P_z^*)}{(P_i^* - P_z^*)}$	$\overline{q}_s^{T\to z}$ (gm/kg)	$\overline{(q_s+Q)}^{T\to z}$ (gm/kg)	$\overline{q}_s^{i\to z}$ (gm/kg)	$\overline{(q_s+Q)}^{i\to z}$ (gm/kg)	$\frac{\overline{(q_s+Q)}^{T\to z}}{[\overline{q}^{+} - \overline{(q_s+Q)}^{i\to z}]}$	$\frac{(\overline{F_w}^{kTt}\Delta t)}{(\overline{P_o}^{kT}\Delta t)}$
100	0.637	1.60	2.35	4.18	4.93	0.259	0.165
150	0.607	1.82	2.57	4.52	5.27	0.295	0.179
200	0.571	2.10	2.85	4.93	5.68	0.343	0.196
250	0.528	2.47	3.22	5.41	6.16	0.411	0.217
300	0.476	2.92	3.67	5.95	6.70	0.502	0.239
350	0.410	3.43	4.18	6.53	7.28	0.622	0.255
400	0.326	4.00	4.75	7.16	7.90	0.780	0.254
450	0.213	4.62	5.37	7.82	8.57	0.989	0.210
500	0.056	5.25	6.00	8.50	9.25	1.26	0.070
514	0	5.40	6.15	8.70	9.45	1.35	0

[1] P_i = 750 mb; P_T = 514 mb; $\overline{q}^{+}$ = 14.0 gm/kg; Q = 0.75 gm/kg; τ = 22°C

(2) Converting the heights to pressure by means of figure 8.

(3) Reading the flux ratio from the steady-state curves in figure 10 at these pressures.

The resulting profiles of flux ratios are shown in figure 13. The curves are labeled in terms of the lowest quintile of cloud heights, 10 percent, through 90 percent, the highest, as in figure 11. Also shown is the mean of these quintile curves.

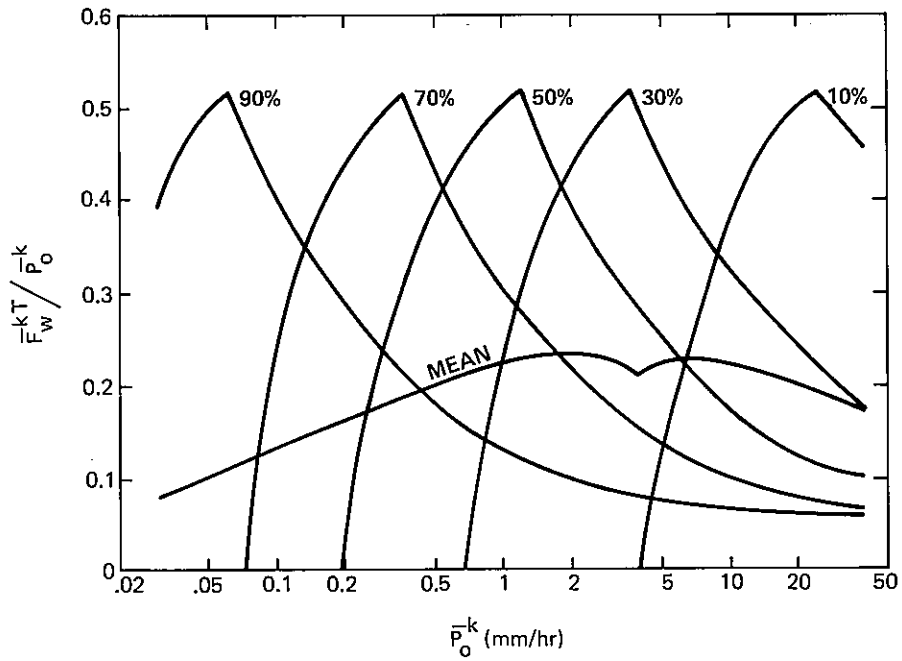

Figure 13.--Steady-state moisture flux ratio vs. rainfall rate. Basic parameterization.

8.4 Significant Rainfall Rates

The percentage contribution of various rainfall rates, as statistically estimated from radar echo lengths, is shown in table 7 for selected representative fair and disturbed days. The table is based on the following:

(1) Census of echo lengths from plan-position-indicator (PPI) scope photographs at equal time intervals.

(2) Average rainfall rate per echo as function of length from Hudlow's (1971) statistical relationship.

(3) Echo area as statistical function of length (Hudlow, 1971).

(4) Rainfall rate times area times time interval between photographs equals echo rainfall volume.

(5) Accumulating total volume and forming class interval percentages.

As seen in table 7, on disturbed days 77 percent of the rain falls at rates of less than 2.89 mm/hr and 98 percent at rates of less than 7.16 mm/hr. These are averages over echo area.

Table 7.--Rainfall rate over echo areas vs. percentage contribution to total rain within 100 mi of Barbados radar for selected days.

Echo length (mi)	Rainfall rate (mm/hr)	Fair days (June 22-26)	Disturbed days (June 27-29)
0 - 10	0 - 0.47	38%	20%
10 - 20	0.47 - 1.16	28%	22%
20 - 30	1.16 - 1.98	17%	18%
30 - 40	1.98 - 2.89	7%	17%
40 - 50	2.89 - 3.87	10%	8%
50 - 80	3.87 - 7.16		13%
over 80	over 7.16		2%
		100%	100%

8.5 Recommendation

The average flux ratio curve in figure 13 for the steady state is relatively flat over the range of important rainfall rates, as is the growth-stage curve in figure 10 in relation to cloud height. Use of 0.22 as the basic average flux ratio for all rainfall rates and periods in BOMEX budget analyses is therefore recommended. The variation of the flux ratio with rainfall rate and between growth stage and steady state does not appear to be great enough to warrant more detailed calculations.

9. FLUXES THROUGH THE TOP OF THE BOMEX VOLUME PER MILLIMETER OF RAINFALL

9.1 Moisture Flux

At the rainfall rates that contribute the largest volume of rain, $\overline{F}_w^{kT}/\overline{P}_o^{k}$ (fig. 13) and $\overline{F}_w^{kTt}\Delta t/\overline{P}_o^{kt}\,\Delta t$ (fig. 10) approximate 0.22. Thus we assume that for each millimeter of rainfall, 0.22 mm of water is exported by clouds through the top.

9.2 Mass Flux

Substituting the values

$$\overline{P}_o^B = 0.1 \text{ gm cm}^{-2} \text{ day}^{-1},$$

$$\overline{q}^{+c} = 0.014 \text{ gm/gm, and}$$

$$\overline{F}_w^{cT}/\overline{P}_o^c = 0.22$$

in eq. (32) gives

$$\frac{\overline{\omega^*}^{cT}}{g} \frac{A_c}{A_B} = \frac{0.1}{0.014} (1+ 0.22) = 8.7 \text{ gm cm}^{-2} \text{ day} \quad .$$

In other words, each millimeter of rainfall (per square centimeter) requires the export of 8.7 gm cm^{-2} of air. This ratio is not area dependent. Each gram of rain requires the export of 87 gm of air, under BOMEX conditions.

9.3 Vertical Velocity

The vertical velocity correction is 8.7 gm x 980 cm s^{-1} = 8,500 microbars day^{-1} = 8.5 mb day^{-1}. This is the upward velocity $\overline{\omega^*}^{BT}$ to be applied to the BOMEX square for each millimeter of rainfall per day, and would be the solution of eq. (8) if $\overline{\omega^*}^{aT}$ were negligible.

9.4 Enthalpy Flux

The right-hand term of (44) now is

$$\left[\frac{\overline{\omega^*}^{cT}}{g} \frac{A_c}{A_B}\right] c_p \Delta T' = 8.7 \text{ x } 0.24\Delta T' = 2.09\Delta T' \text{ cal cm}^{-2} \quad ,$$

which means that each millimeter of rain requires for the model conditions the export of 2.09 cal cm^{-2} <u>per degree temperature difference between cloud</u> and environment, or 0.209 cal cm^{-2} per 0.1° temperature difference. This is the net enthalpy flux in clouds, averaged over the BOMEX square, to be applied as a correction to the average flux calculated from $\overline{\omega^*}^{BT}/g\ c_p\ \overline{T}^{aT}$.

ACKNOWLEDGEMENTS

The problem dealt with in this memorandum was originally suggested by the late Arnold Glaser, former Deputy Director of BOMAP, the predecessor of the Center for Experiment Design and Data Analysis (CEDDA). Helpful discussions were held with many CEDDA colleagues. Specific acknowledgements are due Jason Ching for the Discoverer environmental sounding, Wolfgang Scherer for table 7, and John Jalickee for the analysis on which figure 11 is based.

REFERENCES

Ackerman, Bernice, "Some Observations of Water Contents in Hurricanes," Journal of the Atmospheric Sciences, Vol. 20, No. 4, 1963, pp. 288-298.

BOMAP Office, BOMEX Field Observations and Basic Data Inventory, National Oceanic and Atmospheric Administration, U.S. Department of Commerce, Rockville, Md., 1971, 428 pp.

Davidson, Ben, "The Barbados Oceanographic and Meteorological Experiment," Bulletin of the American Meteorological Society, Vol. 49, No. 9, 1968, pp. 928-934.

Holland, J.Z., and E.M. Rasmusson, "Measurements of the Atmospheric Mass, Energy, and Momentum Budgets Over a 500-Kilometer Square of Tropical Ocean," Monthly Weather Review, Vol. 101, No. 1, January 1973, pp. 44-55.

Hudlow, M.D., "Weather Radar Investigations on the BOMEX," Research and Development Technical Report, ECOM-3329, U.S. Army Electronics Command, Fort Monmouth, N.J., September 1970, 106 pp.

Hudlow, M.D., "Three-Dimensional Model of Precipitation Echoes for X-Band Radar Data Collected During BOMEX," BOMEX Bulletin No. 10, The BOMAP Office, National Oceanic and Atmospheric Administration, U.S. Department of Commerce, Rockville, Md., June 1971, pp. 51-63.

List, Robert J., Smithsonian Meteorological Tables, 6th revised edition, Smithsonian Institution, 1951.

Rasmusson, E.M., "Mass, Momentum, and Energy Budget Equations for BOMAP Computations," NOAA Technical Memorandum, ERL BOMAP-3, the BOMAP Office, National Oceanic and Atmospheric Administration, U.S. Department of Commerce, Rockville, Md., 1971, 32 pp.

Sanders, D., J. Sullivan, and P. Pytlowany, "Correction of BOMEX Radiosonde Humidity Errors," paper presented at Eighth Technical Conference on Hurricanes and Tropical Meteorology, American Meteorological Society, Key Biscayine, Fla., May 1973.

Scherer, W.D., and M.D. Hudlow, "A Technique for Assessing Probable Distributions of Tropical Precipitation Echo Lengths for X-Band Radar From Nimbus 3 HRIR Data," BOMEX Bulletin No. 10, The BOMAP Office, National Oceanic and Atmospheric Administration, U.S. Department of Commerce, June 1971, pp. 63-68.

Scherer, W.D., and M.D. Hudlow, BOMEX Period III Radar-Satellite Atlas, Center for Experiment Design and Data Analysis, National Oceanic and Atmospheric Administration, U.S. Department of Commerce, Washington, D.C., 1975, in press.